

INVESTIGATION OF X-RAY HARMONICS IN THE POLARIZED NONLINEAR INVERSE COMPTON SCATTERING EXPERIMENT AT UCLA

O. Williams, A. Doyuran, R.J. England, C. Joshi, J. Lim, J.B. Rosenzweig, S. Tochitsky, G. Travish

UCLA Department of Physics and Astronomy/Department of Electrical Engineering
Los Angeles, CA 90095, U.S.A.

Abstract

An Inverse Compton Scattering (ICS) experiment investigating the polarized harmonic production in the nonlinear regime has begun which will utilize the existing terawatt CO₂ laser system and 15 MeV photoinjector in the Neptune Laboratory at UCLA. A major motivation for a source of high brightness polarized x-rays is the production of polarized positrons for use in future linear collider experiments. Analytical calculations have been performed to predict the angular and frequency spectrums for various polarizations and different scattering angles. We report the set-up and experimental status. The advantages and limitations of using a high laser vector potential, a_0 , in an ICS-based polarized positron source are expected to be revealed with further measurement of the harmonic spectrum and angular characteristics.

INTRODUCTION

The production of 3rd generation light source quality x-rays using low energy electron beams has spurred much interest in ICS as well as the possibility of using it as a source of polarized positrons in high energy physics experiments. This requires an understanding of the nonlinear and polarization properties of the scattering process during high laser intensities ($a_0 \geq 1$).

The spectral and angular distribution of the nonlinear scattering process has yet to be determined experimentally and it is unknown whether the laser polarization is conserved during the nonlinear interaction. The physics behind this scattering mechanism should give more insight into the limitations of using a laser or other electromagnetic field as an undulator for the production of x-rays.

The Neptune Laboratory at UCLA houses a terawatt-class CO₂ laser system capable of achieving $a_0=1$. This is the necessary condition to obtain nonlinear scattering and hence higher harmonic generation. Very strong focusing is therefore required at the interaction point (IP) for both the laser and electron beam. In order to focus the (design) 14 MeV, 300 pC, low emittance beam produced by the 1.6 cell S-Band photoinjector and linac, the development of an array of ultra-strong focusing permanent magnet quadrupoles (PMQ's) was necessary. The short laser focal length and small aperture of the PMQ's necessitated

a transverse (90°) scattering geometry between the laser and electron beam.

EXPERIMENTAL SET UP

The layout of the interaction region is shown in Figure 1. In order to obtain rms beam sizes near 25 μm, strong focusing is required. To achieve this, PMQ's were developed with a gradient of ~115 T/m. Five total PMQ's are arranged in a modified triplet configuration (FF-DD-F) with 1.5 cm to the minimum beam waist (IP), followed by a symmetric triplet for recollimation. Both PMQ assemblies are manually adjustable with respect to the IP and remotely together to allow scanning of the waist along the beam axis.

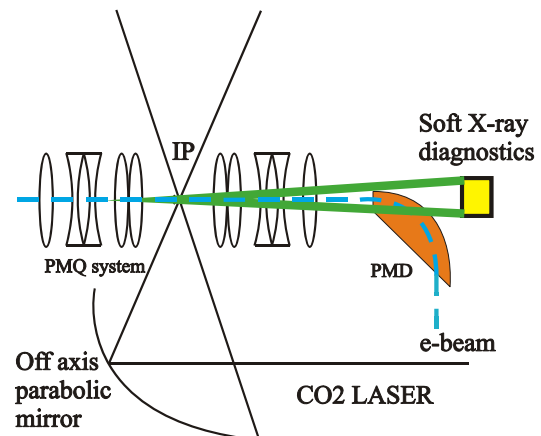


Figure 1: Experimental layout of the interaction region.

It can be seen in the expression for the laser vector potential, $a_0 = \lambda_L e E_L / 2\pi m_e c^2$, that longer wavelength light makes a_0 large, giving an advantage to CO₂ lasers. However, a high intensity spot is still required at the IP and for 500 GW of 10.6 μm light, this necessitates a 25 μm spot (RMS). This strong focusing is accomplished by a 5" copper off-axis parabolic mirror with an F# of 1.5 oriented 90° with respect to the beam axis, resulting in orthogonal scattering with the electron beam. The design parameters for the electron and laser beams are shown in Table 1.

Table 1: Design Electron and Laser Beam Parameters

Parameter	Value
Electron Beam Energy	14 MeV
Beam Emittance	5 mm-mrad
Electron Beam Spot size (RMS)	25 μm
Beam Charge	300 pC
Bunch Length (RMS)	4 ps
Laser Beam radius at IP (RMS)	25 μm
CO ₂ Laser Wavelength	10.6 μm
CO ₂ Laser Rayleigh Range	0.75 mm
CO ₂ Laser Power	500 GW
CO ₂ Laser Pulse Length	200 ps

Because the scattered light is emitted in a forward cone of half angle θ , similar to synchrotron light, it is inversely proportional to the electron beam energy ($\theta \sim 1/\gamma$) and for our case of $\gamma \approx 28$, $\theta = 15$ mrad (see Table 2 for more scattered photon parameters). This large angle imposed strong space constraints on the experimental layout. In order to place the x-ray diagnostics (i.e. x-ray CCD camera) as close to the source as possible to fully image any off-axis harmonics, the electron beam needed to be bent and dumped immediately following recollimation. The strong bend required a very powerful, compact, permanent magnet dipole (PMD).

Table 2: Calculated Scattered Photon Parameters

Parameter	Head-on	Transverse
Scattered photon wavelength	5.3 nm	10.7 nm
Scattered photon energy	235.3 eV	117.7 eV
Scattered photon pulse duration (FWHM)	10 ps	10 ps
Interaction time	5 ps	0.33 ps
# of periods electrons see	283	10
# of photons emitted per electron	3.34	0.11
Total # of photons	6.3×10^9	2×10^8
Half Opening Angle (θ)	2.7 mrad	15 mrad
Bandwidth	0.35%	10 %

Permanent Magnet Quadrupole (PMQ)

The PMQ's are constructed using commercially available, $M=1.2$ T, NdFeB cubes supported in a hexagonal iron yoke with hyperbolic iron tips about the beam axis. An aluminum spacer is used to constrain the individual cubes within the yoke, as shown in Figure 2. To assure a uniform, magnetic-to-mechanically matched field about the beam axis, the hyperbolic tips, yoke, and aluminum spacer are electric discharge machined (EDM) for better precision and the cubes measured with a hall probe and sorted. Using the pulse wire method, the magnetic axis was found to be within 25 μm of the geometric axis.

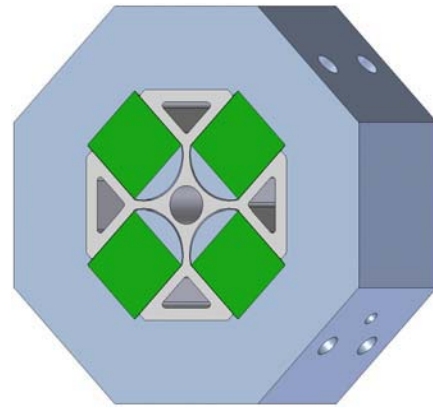


Figure 2: PMQ design using 4 cube magnets, hyperbolic pole tips and aluminum spacers.

Permanent Magnet Dipole (PMD)

The PMD is shown in Figure 3. The size of the gap had to be considered not only for desired field strength, but also because too small of a gap could clip the scattered photons. The resultant design included $M=1.32$ T, NdFeB magnets cut circularly to optimize scattered photon transport and a 16 mm gap, yielding a dipole field of ~ 0.78 T/m. This produces a bend radius of 60 mm for 14 MeV electrons. Field measurements are in excellent agreement with Radia3D simulations. To accommodate off-energy and off-trajectory particles, the PMD has been placed on a heavy load in-vacuum actuator which translates vertically. Changing the position at which the electrons enter the PMD correspondingly changes their exit position and angle. This allows for acceptance of 12-14 MeV beams with transverse offsets and entrance angles.

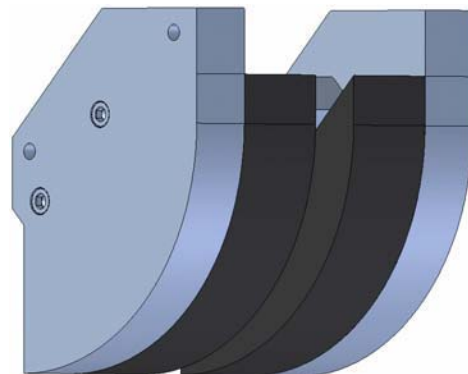


Figure 3: Compact dipole using permanent magnets. The beam enters from the left and is bent 90° upwards.

IP Diagnostics

The spatial overlap and synchronicity of arrival at the IP between the electron and laser beam is critical to obtain sufficient flux of scattered photons. The high density of charge in the 25 μm electron spot at the IP makes traditional YAG or phosphor imaging less desirable due to limited spatial resolution [2]. Therefore, we chose to

image the electron beam using optical transition radiation (OTR). The difficulty of imaging a 90° interaction is also complicated by the compactness of the experiment and transport of light at the IP intended for alignment diagnostics. This prompted the development of a highly reflective, sharp-edged, aluminum pyramid used to simultaneously image the two beams as seen in Figure 4.

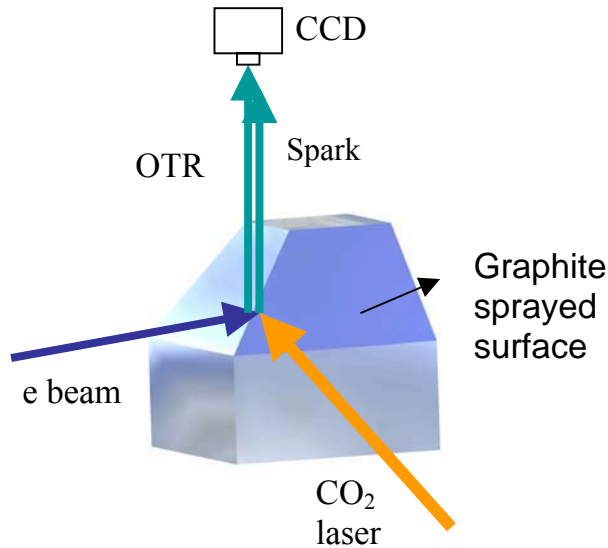


Figure 4: The IP imaging diagnostic “pyramid”.

The $10.6\ \mu\text{m}$ light, not lying in the visible spectrum, requires the application of a thin layer of micron-sized graphite on the laser imaging surface of the pyramid which “sparks” when hit by the laser, allowing for both beams to be overlapped along the pyramid’s edge as imaged by a vertically mounted CCD camera.

The two beams must also be synchronized in time at the IP. This is accomplished through a Germanium crystal acting as a “gate”. When the beam electrons are incident on the crystal oriented at 45° , a semiconductor plasma is formed which is opaque to the $10.6\ \mu\text{m}$ laser light. By measuring the transmitted intensity of the laser, the relative timing between the beams is revealed and allows for tuning of the arrival time at the IP.

X-ray Imaging

Two types of x-ray imaging devices are planned for use in the experiment, a soft x-ray CCD camera (on loan from the ANL APS) and a microchannel plate (MCP). The x-ray camera will be used to image primarily the beam axis with good resolution. Because the x-ray source is diverging so strongly and the x-ray camera has an imaging area of only $12.3 \times 12.3\ \text{mm}^2$, it resides in a reentrant housing allowing it to be inserted in the vacuum chamber, closer to the source.

The MCP detector has a 40 mm diameter imaging area and is mounted further from the source than the x-ray camera, yet still has 75% more field of view. After being

cross-calibrated against the x-ray camera, the MCP will be used to better image the beam off-axis, particularly the expected higher harmonics.

Calculation Tool

A Mathematica routine has been developed which predicts the angular and frequency spectra for the scattered photons at different scattering angles and laser polarizations. Shown below in Figure 5 are the expected photon distributions for the fundamental at a scattering angle of 90° and σ and π polarizations. More detailed literature on higher harmonics for head-on scattering can be found in Ref. 3, while the transverse case is part of ongoing work.

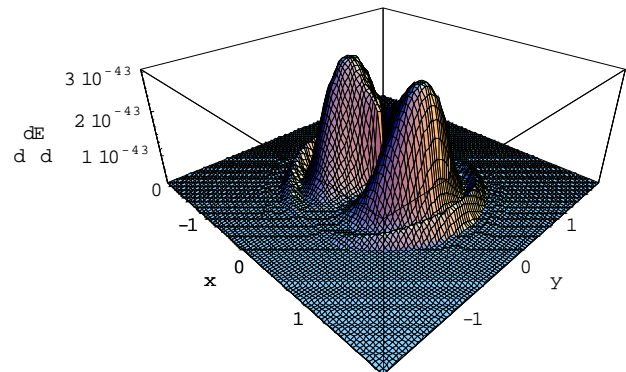
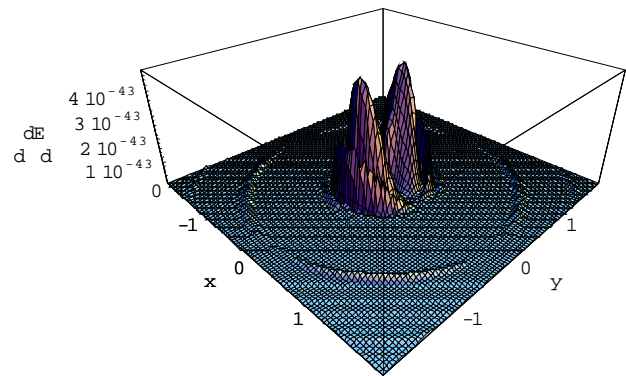


Figure 5: Intensity plot of σ (a) and π (b) polarizations at first harmonic. The screen location is set $z=\gamma$ and x and y are in mm units.

STATUS OF THE EXPERIMENT

Transverse profile measurements of the laser beam at the IP have been made using a pyrocam. The minimum waist size was found to be $\sim 60\ \mu\text{m}$ and is shown in Figure 6.

The diagnostic pyramid and motion devices have been installed in the box and initial alignment of the electron and laser beams at the IP is beginning. Preliminary x-ray background tests with both beams operating are also

starting and are expected to help optimize the shielding surrounding the detector.



Figure 6: Transverse profile of the laser beam at the IP. Minimum beam waist found to be $\sim 60 \mu\text{m}$.

REFERENCES

- [1] A. Doyuran, et al., Study of X-ray Harmonics of the Polarized Inverse Compton Scattering Experiment at UCLA, AAC 2004 Proceedings.
- [2] A. Murokh, et al., Limitations on Measuring a Transverse Profile of Ultra-Dense Electron Beams with Scintillators, PAC 2001 Proceedings.
- [3] G.A. Krafft, Spectral Distributions of Thomson-Scattered Photons from High-Intensity Pulsed Lasers, PRL Vol. 92 p 204802.